

Research on the inverse kinematics prediction of a soft biomimetic actuator via BP neural network

Huichen Ma¹, Student Member, IEEE, Junjie Zhou², Jian Zhang¹, and Lingyu Zhang^{1,2}

¹School of Mechanical Engineering, Beijing Institute of Technology, Beijing 100081, China.

²Institute of Advanced Technology, Beijing Institute of Technology, Tsinan 250300, China.

Corresponding author: Junjie Zhou (e-mail: bit_zhou50082@163.com).

This work was supported by the National Key Laboratory of Vehicular Transmission of China (grant number JCKYS2019208005).

ABSTRACT Inspired by the pneumatic artificial muscle, soft biomimetic pneumatic actuators have been applied in many applications due to their high flexibility, good environmental adaptability, and safe interaction with the surroundings. In this work, we address the inverse kinetics problem of motion planning of soft biomimetic actuators driven by three chambers. Although the mathematical model describing the inverse dynamics of this kind of actuator has been employed, this model is still a complex system. On the one hand, the differential equations are nonlinear. Therefore, it is complicated and time-consuming to get analytical solutions. Since the exact solutions of the mechanical model are not available, the elements of the Jacobian matrix cannot be calculated exactly. On the other hand, the material model is a complicated system with significant nonlinearity, non-stationarity, and uncertainty, making it challenging to develop an appropriate system model. To overcome these intrinsic problems, we propose a back-propagation (BP) neural network learning the inverse kinetics of the soft biomimetic actuator moving in three-dimensional space. After training with sample data, the BP neural network model can represent the relation between the manipulator tip position and the pressure applied to the chambers. The proposed algorithm is very precise and computationally efficient. The results show that a desired terminal position can be achieved with a degree of accuracy of 2.46% relative average error with respect to the total actuator length, demonstrating the ability of the model to realize the inverse kinematic control of the soft biomimetic actuator.

INDEX TERMS Soft Actuator, Multiple degrees of freedom, Omnidirectional bending, Mechanical Modeling, Experiment

I. INTRODUCTION

There have been expanding interests and increasing advancements of soft robots in recent years. Compared with traditional rigid robots, soft robots have irreplaceable advantages due to their intrinsic softness, such as high flexibility, good environmental adaptability and safe interaction with the surroundings, etc. [1, 2]. They play an irreplaceable role in the development of society. Therefore, soft robots could make a significant impact in many areas, including industrial applications[3], medical rehabilitation training devices[4], and bionic robots[5, 6].

Soft biomimetic actuators (SBAs) with internal fluidic channels are moved by the fluid and made of hyperelastic materials, which deform upon the pressurization of the internal channels to generate moving[7, 8]. The motion response of SBAs is governed by their morphology, which is

defined by the geometry of the internal fluidic channels and the material properties used in fabrication. During the fabrication of SBAs, carbon fiber reinforced plastic is added to constrain the motion posture and significantly improve their strength, resulting in bending motion similar to human fingers and arms[9]. Therefore, as SBAs are used as soft biomimetic robotic arms and soft biomimetic robotic fingers, different structure designs and drive pressures will produce multistate 2D and 3D movements.

With the development of new material technologies, many materials have been studied and applied to SBAs[10]. Onal *et al.* used hyperelastic materials such as soft silicone rubber material to mold a soft octopus arm[11]. Zhang *et al.* proposed a paradigm to design and manufacture a fast-response, stiffness-tunable (FRST) soft biomimetic robotic gripper driven by shape memory polymer (SMA)[12]. Laschi

et al. developed an actuation mechanism for continuum robotic arms by combining cable and SMA[13, 14]. Xu *et al.* presented a soft bio-inspired annelid robot via dielectric elastomer actuators (DEAs) [15]. A complete overview of works related to materials in soft robots can be found in Laschi *et al.*[16].

The main challenge in building a soft biomimetic actuator is the control of such highly flexible structures. Compared with rigid robotic actuators, it is difficult to accurately model and control the forward and inverse kinematics of SBAs due to both material and geometric nonlinearities. For SBAs, the solution of the inverse kinematics problem is essential to generate paths in the task space in order to perform grasping or other tasks. It is a challenging task to solve the inverse kinematics. As for the research on inverse kinematics modeling and characterization of SBAs, previous efforts can be classified into two groups: 1) model methods and 2) model-free methods.

Model methods follow analytical or numerical approaches[17-19]. The tradeoff between computing time and accuracy needs to be made when applying a model method[20]. For continuum SBAs, just like for rigid robots, we can differentiate the direct kinematics model to find the manipulator tip position kinematics model, i.e., the linear transformation of the tip position velocity into the actuation variables velocity. Subsequently, in order to improve the prediction accuracy of the model, the kinematics of soft robots are mainly derived based on the piecewise constant curvature approximation[21]. Furthermore, many of the dynamics used either Euler/Lagrange or Lagrange formulations with quasi-static simplification [22-24]. The linear transformation is realized by the Jacobian matrix. These models may not accurately capture the complex nonlinear dynamics of soft robots. In part, specific approximations and assumptions of shape are required, and the computational hardness of the Jacobian matrix needs to be solved[25]. In the second place, an accurate material property model is needed. When SBAs are made of different materials, designed for complex structures, or added embedded components, the theoretical model will become more complex. A more complex model may solve these problems, but the process of deriving such models is tedious and brings some difficulty to the calculation[26-28]. Thus, due to the assumptions in the reduced model, the progressive computation accumulates numerical errors along with time steps, which brings in the accuracy problem for the SBA deformation.

The aforementioned challenges can be tackled via model-free methods based on machine learning approaches. The machine-learning and computer vision are mainly applied to model-free methods. Initial research into combining soft robotics with machine learning approaches can be traced back to Elgeneidy *et al.* [29], who applied a purely data-driven approach for modeling the bending of soft pneumatic actuators. In addition, Van Meerbeek *et al.*[30] proposed

various machine learning techniques to predict the type and magnitude of deformation in terms of twisting and bending of soft optoelectronic sensory foams with proprioception. Apart from that, only a few researchers consider using a long short-term memory (LSTM) network and feed-forward neural (FFN) network as the kinematic and force model[7, 16, 31, 32]. Nonetheless, these works did not address the issue of inverse dynamics of soft actuators, that is, the ability to estimate the input signal according to the moving state of actuator systems.

In order to further analyze and solve the inverse kinematics problem of SBAs, this paper combines the soft biomimetic actuator and BP neural network algorithm. The main contributions of this work are summarized as follows.

1) Based on the BP neural network algorithm, a complete soft biomimetic actuator inverse kinematics framework that can predict the driving pressures of the SBA on curved trajectories is established.

2) Solve the model, and find the optimal parameters of the computing framework without exceeding the accuracy constraint.

3) In the trajectory planning experiment, trajectory errors are solved and analyzed, and it is found that average position error, maximum position error, and standard deviation are less than those of the traditional analytical method.

II. METHODS

A. MODELLING BASED ON BP NEURAL NETWORKS

BP neural network is a kind of multilayer feed-forward with forward information propagation and error back-propagation. Compared with the traditional curvature approximation method, the BP neural network method is more suitable for processing nonlinear and complex system problems, preferably due to its complex self-learning and adaptive capabilities, which can greatly increase the fitting accuracy. And it does not need to filter and denoise the experimental data. Thus, we propose a BP neural network architecture based on finite experimental data of tip coordinates of the soft actuator. This architecture could efficiently implement the prediction of the soft actuator motion. The BP neural network is a three-layer network that utilizes the connection weight to store information and fit functions. The layers contain the input layer, hidden layer, and output layer. And each layer has a series of nodes. The structure diagram of the BP neural network is presented in Fig. 1. The connection weights are expressed as ω_{ij} and ω_{jk} , which denote the weight from input node i to hidden node j and hidden node j to output node k , respectively. In the error reverse propagation algorithm, the BP neural network adjusts the weights and thresholds continuously to approximate an arbitrary nonlinear function until obtaining a satisfactory output. Assume that the input

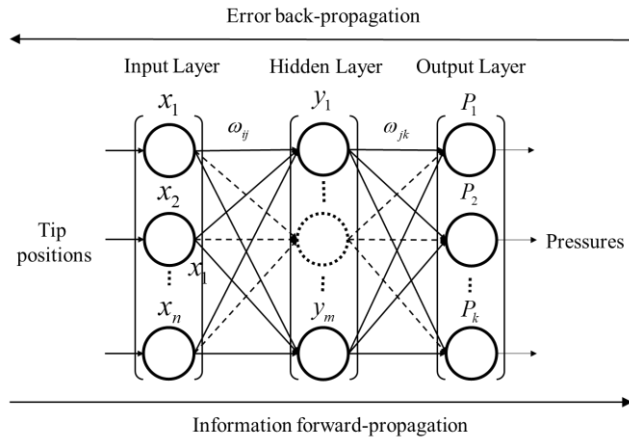


FIGURE 1. The structure diagram of a BP neural network.

value is x_i , $i = 1, 2, \dots, n$, the outputs of the hidden layer are calculated at first[33],

$$y_j = f_1 \left(\sum_{i=1}^n \omega_{ij} x_i + b_j \right) j = 1, 2, \dots, m \quad (1)$$

where y_j denotes the output of hidden node j , b_j represents the bias of hidden node j , m stands for the number of hidden nodes, and f_1 is the activation function of the hidden layer. Then the output value is computed as follows,

$$P_k = f_2 \left(\sum_{j=1}^m \omega_{jk} y_j + \beta_k \right) k = 1, 2, \dots, p \quad (2)$$

where P_k represents the output of output node k , β_k represents the bias of output node k , p stands for the number of output nodes, and f_2 is the activation function of the output layer.

The global prediction error E is trained to achieve the minimum value via the back-propagation algorithm.

$$E = \frac{1}{2} \sum (P_k - R_k) \quad k = 1, 2, \dots, p \quad (3)$$

where R_k is the real output data.

In the current study, the sigmoid function is used for nonlinear relationships and represents an activation function for the respective neural layer. It has the advantages of being smooth, continuous, and differentiable and is more accurate than the linear function. In addition, the sigmoid function is not sensitive to the noise generated in learning, which can reflect the mainstream direction of a large number of data samples. By using sigmoid hidden neurons, the nonlinear mapping from the tip coordinates (x, y, z) of the soft actuator to the input pressures is established, that is,

$$(P_1, P_2, P_3) = f(x, y, z) \quad (4)$$

B. PARAMETERS OF THE BP NEURAL NETWORK

The number of nodes of the input layer is the number of the tip coordinates (x, y, z) , and therefore, the number of input nodes is 3. We predicted the input pressures (P_1, P_2, P_3) of three chambers simultaneously, and therefore, the number of output nodes is 3.

The node number of the hidden layer affects the capacity of the BP network a lot: if the number of nodes is too small, it is less likely to produce the network with low precision; on the contrary, it is prone to oscillation and minimum local phenomenon may appear. In this paper, we use the empirical formula to calculate the number of hidden layer neurons in the first training process, train and compare the different numbers of neurons, and thus derive the optimal neuron number of the hidden layer[34, 35].

$$N_{\text{hid}} = \sqrt{N_{\text{in}} + N_{\text{out}}} + \alpha \quad (5)$$

where N_{hid} is the number of hidden layer neurons; N_{in} and N_{out} are the input node number and the output node number, respectively. α is a constant between 1-10.

Since the BP neural network model is a 3-input 3-output model, the number of hidden layer neurons ranges from 3 to 13. Even if the same number of hidden layer neurons are trained by using the same data, the output results may be different for the uncertainty and complexity of the network. Therefore, the optimum neurons in the hidden layer of the network are determined by the method of trial and error in this study. Regression-coefficient (R) is frequently used to measure the differences between the values predicted by a model or an estimator. If a good model is expected, R^2 must be close to 1.

Fig. 2 shows the training and verification results of a different number of neurons in the hidden layer, and it is found that the training error is the smallest when the hidden layer has 13 neurons. The mean value and median level under this number of neurons in the hidden layer are also the highest, representing that the network under this hidden neuron number is more stable. Then the network structure of the model is determined to be 3-13-3.

In order to avoid overfitting and falling into a local minimum, three parameters of the BP neural network structure are chosen: the training time N_T that the algorithm is repeated, the training precision N_P , and the learning rate N_L that determines the size of the step.

Training precision is set to 0.01 to meet the motion accuracy requirement of soft robots. The learning rate needs to be determined in Matlab. Different learning rates can be selected for training, and the learning loss function results are shown in Fig. 3(a). The loss function doesn't improve when the learning rate is too low. The loss function begins to diverge if the learning rate is too high. Thus, the best learning rate is finally determined to be 0.01. Record its mean squared error after every 10 iterations, and observe its

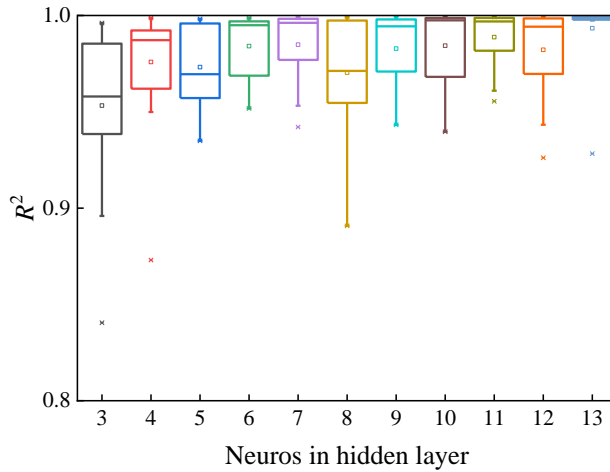


FIGURE 2. The R^2 values of different neuron numbers in the hidden layer.

convergence. As shown in Fig. 3(b), when the number of iterations is 500, the algorithm starts to converge, after which it remains stable, reaching the training precision value of 0.01. This shows that the algorithm model has a faster convergence speed. The number of iterations is 500.

- $N_T = 500$
- $N_P = 0.01$
- $N_L = 0.01$

After determining the number of hidden layer neurons, the data set is divided into the training set and the testing set. The data under the chamber 1 pressure of 0 MPa, 0.8 MPa, and 1.6 MPa serves as the training set. The data under the chamber 1 pressure of 0.4 MPa, 1.2 MPa, and 2.0 MPa serves as the testing set. The training set is used during the learning phase, whereas the testing set is only employed to evaluate the performance of the BP neural network model.

C. MODEL ERROR ANALYSIS

The training set is used to train the BP neural network model with a 3–13–3 structure. At the same time, the testing set is used to verify the identification accuracy, as shown in Fig. 4. To evaluate the performance of the model, the mean absolute percentage error (MAPE) is applied. And this metric is defined as follows,

$$MAPE = \frac{1}{N} \sum_{i=1}^N \left| \frac{F_i - T_i}{T_i} \right| \times 100\% \quad (6)$$

where N is the number of test data, F_i is i -th forecast value, and T_i is i -th actual value.

The results show that under different tip positions of the soft actuator, the maximum APE between the test value and prediction value is less than 6%. The MAPE for this model is less than 5%. The R^2 of the prediction model reaches

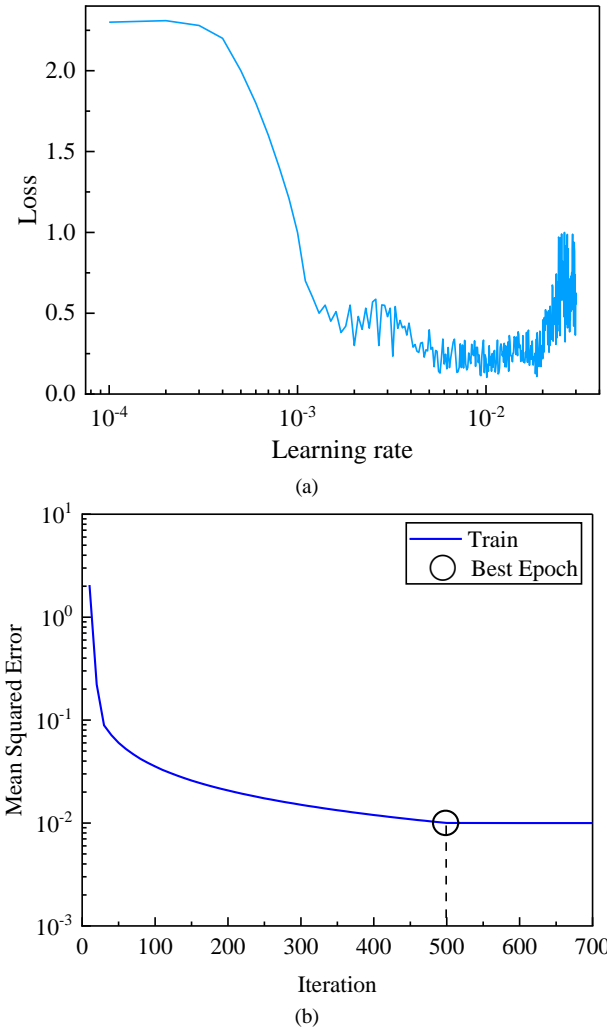


FIGURE 3. (a) Learning rate situation; (b) Best training performance is the iterations of 500 at the learning rate of 0.01.

0.9767, which indicates that the predicted values are in good agreement with the actual values and could meet the prediction requirements of the inverse kinematics and the control demands of soft actuators.

D. ANALYTICAL MODELLING

To verify our modeling approach, we performed the inverse kinematics analytical model[36]. This model conducts the open-loop control of the soft biomimetic actuator's tip position. The structural sketch of the soft biomimetic actuator under deformation is established in Fig. 5. The inverse kinematics process can be decomposed into three steps. The first step relates the tip coordinates (x_0, y_0, z_0) of the SBA to the parameters (l, θ, φ) . The second is the transformation from the parameters (l, θ, φ) to the lengths of chambers (l_1, l_2, l_3) . And the last one is from chamber lengths to the input pressures (P_1, P_2, P_3) .

First, the azimuth angle φ , the bending angle θ , and the axial length l can be obtained from the tip position (x_0, y_0, z_0) as

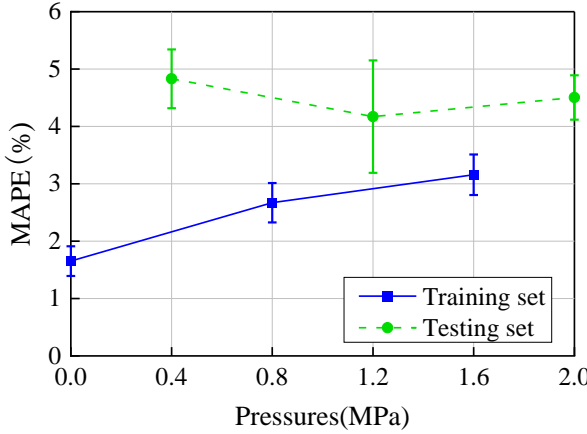


FIGURE 4. The MAPE of the BP neural network model.

$$\varphi = \tan^{-1} \left(\frac{y_0}{x_0} \right) \quad (7)$$

$$\theta = \cos^{-1} \left(\frac{z_0^2 \cos^2 \varphi - x_0^2}{z_0^2 \cos^2 \varphi + x_0^2} \right) \quad (8)$$

$$l = \frac{z_0 \cdot \theta}{\sin \theta} \quad (9)$$

It should be noted that the bending angle θ would be miscalculated as zero when $x = 0$. So, in this case, we need (10) as an auxiliary.

$$\theta = \cos^{-1} \left(\frac{z_0^2 \sin^2 \varphi - y_0^2}{z_0^2 \sin^2 \varphi + y_0^2} \right) \quad (10)$$

Then, the axial lengths of three chambers (l_1 , l_2 , l_3) can be represented with (l , θ , φ).

$$l_1 = l - \theta d \cos \left(\frac{\pi}{2} - \varphi \right) \quad (11)$$

$$l_2 = l - \theta d \cos \left(\frac{7\pi}{6} - \varphi \right) \quad (12)$$

$$l_3 = l - \theta d \cos \left(\frac{11\pi}{6} - \varphi \right) \quad (13)$$

where d is the distance between the center of the soft actuator and the center of each chamber.

For pressures, we have the following description:

$$P_1 = \frac{l_1 / l_0 - (l_0 / l_1)^3}{k} \quad (14)$$

$$P_2 = \frac{l_2 / l_0 - (l_0 / l_2)^3}{k} \quad (15)$$

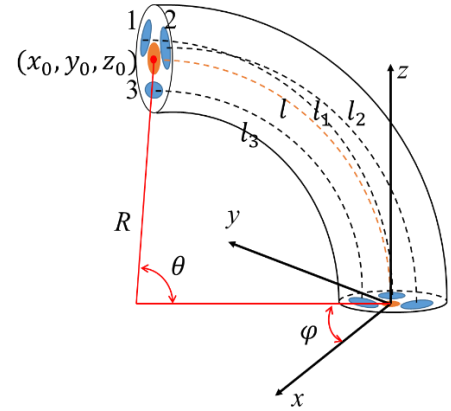


FIGURE 5. The structural sketch of the soft actuator under deformation.

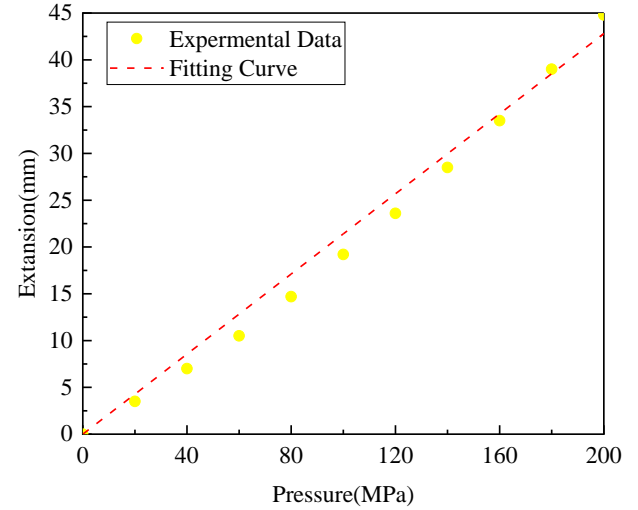


FIGURE 6. The actuator elongation for identifying the initial shear modulus of the SBA.

$$P_3 = \frac{l_3 / l_0 - (l_0 / l_3)^3}{k} \quad (16)$$

where k is given as

$$k = \frac{A}{\mu_0 \cdot A'} \quad (17)$$

where A is the stress area of the air chamber, A' is the projected area of the actuator body material, and μ_0 is the initial shear modulus of the silicone material.

To identify the material parameters μ_0 and k , three chambers are pressurized equally from 0 kPa to 200 kPa at intervals of 20 kPa, and the lengths are recognized. Fig. 6 presents the experimental data and the fitting curve. The parameter k in (17) equals 2.128 MPa^{-1} , and the parameter μ is 0.282 MPa. According to the results, we can calculate the required pressures to the tip coordinates of the soft

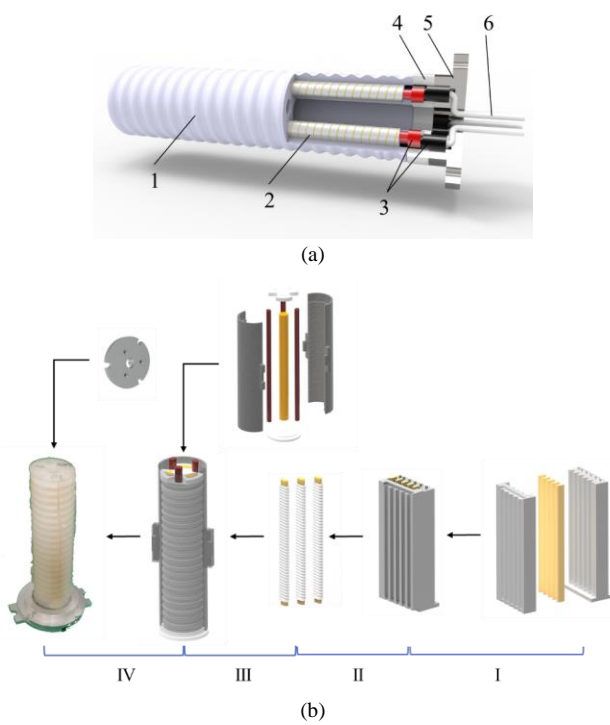


FIGURE 7. Schematic of (a) the soft biomimetic actuator (a) and the fabrication of the soft biomimetic actuator.

actuator through the inverse dynamics model.

III. MATERIALS

A. ACTUATOR DESIGN AND FABRICATION

Fig. 7(a) shows the main structures of the SBA: 1) High elastic silicone driver matrix; 2) Three fiber-reinforced chambers; 3) Pneumatic connectors; 4) High hardness silicone molded sealed cap; 5) A metal base connector; 6) Pneumatic hoses.

The soft actuator is composed entirely of soft materials. The three elastic chambers dispose at 120° apart, and three smaller internal passages are disposed at 120° apart for weight loss. The radial restraint of the three chambers takes the form of left-right symmetrical double spiral fiber winding in this design, and the winding angle of the fiber is $\pm 3^\circ$. In this way, the elastic fiber provides tension along the direction to exert large circumferential stress. When filled with fluid, the elastic air chamber only extends axially. The three chambers connect to different air valves that provide pressurized fluid through a pneumatic hose inserted at the top of each chamber. Afterward, the actuator deforms under the action of three trigonally symmetrical pressurized chambers. When the pressures in the chambers are equal, the chambers elongate to the same length, leading to an axial stretching of the whole actuator. When the pressures in the chambers are not equal, the lengths of the chambers differ from each other, which allows the soft actuator to bend in any direction besides stretching in an axial direction. The metal base connector can be used to match the rigid

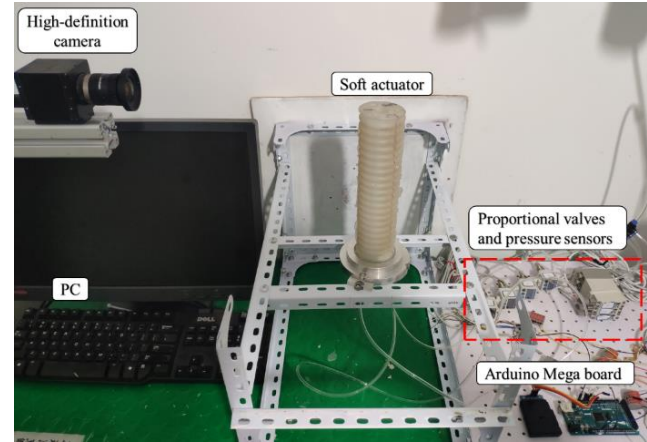


FIGURE 8. Overview of the soft biomimetic actuator experiments setup.

mounting plate on the experimental platform to ensure the stability of the installation. Meanwhile, the connector is designed for expansibility. It can be further stuck to another soft actuator or other modules.

The procedure involved for fabricating the soft actuator can be summarised in the following steps as shown in Fig. 7(b):

I: The mold pressing of the elastic chamber. First, the chamber core and chamber casting mold are 3D printed with ABS material, and the inner layer elastic air chamber with a thickness of 1.5mm is cast with low-hardness silicone. The silicone consists of parts A and B (1A: 1B by weight). Before assembling the molds, the release agent (LW-366, LONG WEI, China) is used to treat the surface of the molds to reduce the adhesion between silicone and ABS molds.

II: The fiber winding. Kevlar fibers are used to envelop the elastic chambers and restrain their radial expansion.

III: Actuator matrix molding. Insert the fiber-reinforced elastic chambers into the positioning hole of the ABS base plate, and cast the main part of the soft actuator with low hardness silicone. After curing, the joint sealed cap part is cast with high-hardness silicone.

IV: The actuator end seal encapsulation. Fix the metal base connector with a silicone adhesive to the actuator matrix after stripping, and finally connect the joint with pneumatic hoses.

B. EXPERIMENTS SETUP

To explore the relationship between the pressure and manipulator tip position and validate the inverse dynamic modeling based on the BP network, we have set up an experimental platform, as shown in Fig. 8.

The soft actuator is driven by a pneumatic driving device which could set pressure of the three chambers via proportional valves (ITV0030-2BL, SMC, Japan). The control algorithm of proportional valves is programmed in Arduino. The timing of the actuation and the effective

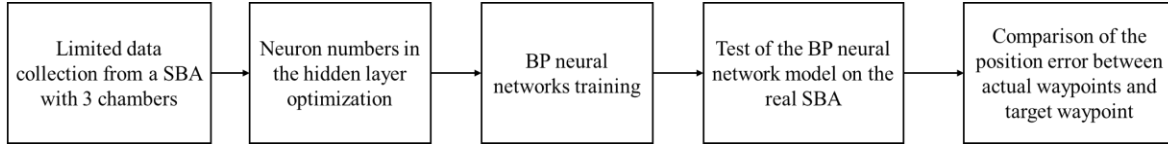


FIGURE 9. The experimental procedure followed in the model application section.

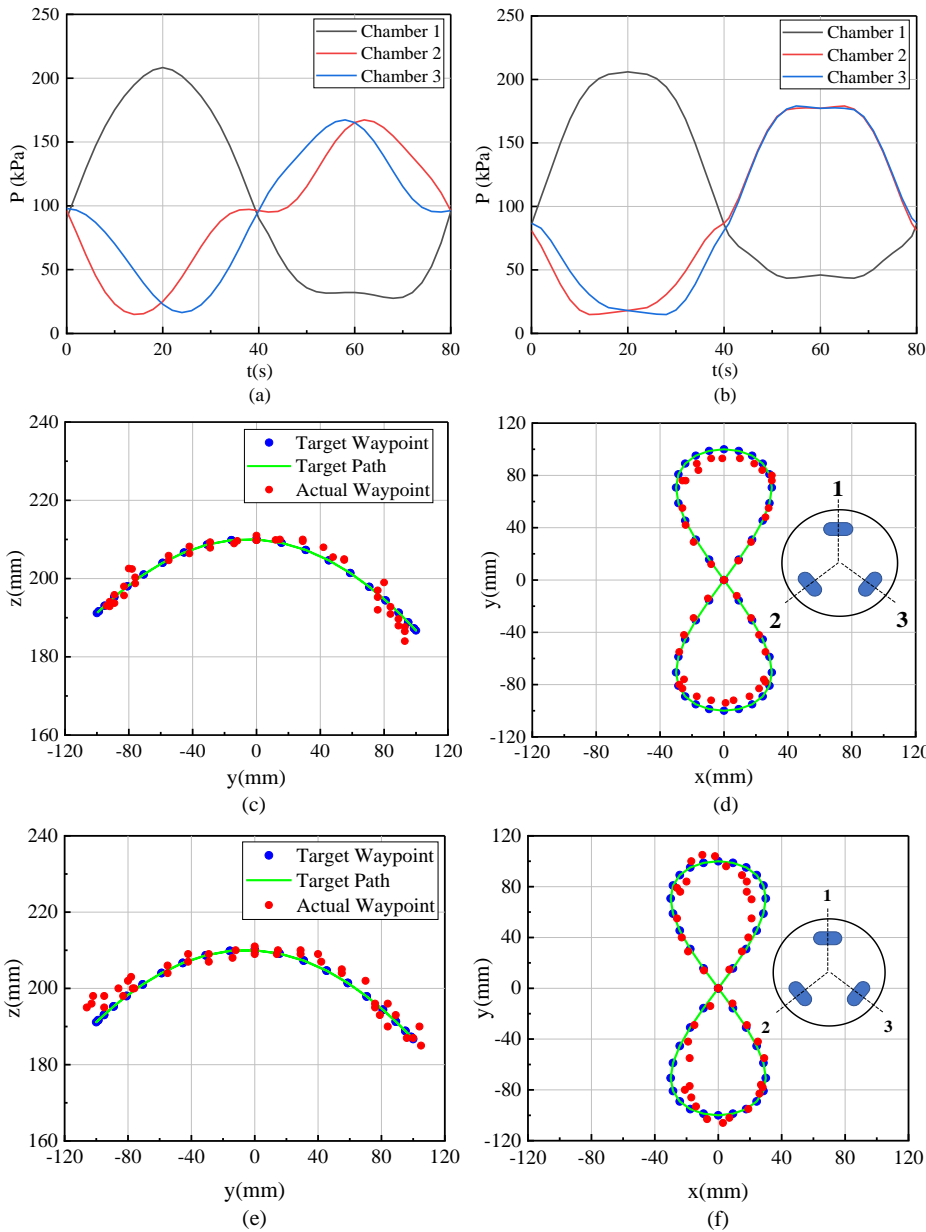


FIGURE 10. Pressure inputs to the three chambers and tip path of the soft biomimetic actuator: (a) Input pressures of BP network prediction model; (b) Input pressures of analytical model. (c) Side view in the BP network model. (d) Top view in the BP network model. (e) Side view in the analytical model. (f) Top view in the analytical model.

pressure supply are implemented through an Arduino Mega board (UNO R3, Arduino, Italy). Three pressure sensors (ISE80H-02-R, SMC, Japan) are used to collect the real-time pressures of the fluid in three chambers. Colored tape is attached to the ends of the soft actuator as a marker to facilitate coordinate recognition. Two high-definition

cameras (MV-VD030SC, Microvision, China) are mounted on the two adjacent walls to collect the tip coordinates of the soft actuator. Finally, the coordinates of the mark points could be measured by a motion analysis software Tracker.

In order to demonstrate the value of the proposed kinematic model, we apply the input pressures to three

chambers in various combinations of 0 kPa to 200 kPa at intervals of 40 kPa and test the tip positions of the soft actuator. In total, 216 pairs of valid data (pressures and tip positions) are obtained.

IV. RESULTS

In detail, the method process is illustrated in Fig. 9. After simple data collection from the SBA bending experiment, the data are used for the neuron numbers in the hidden layer optimization and training of the BP neural network model. Once the parameters of the BP neural network are defined, the inverse kinematics algorithm from the manipulator tip position to the input pressure can be implemented.

To prove the practical value of the BP neural network model, we conduct the model-based open-loop control of the tip positions of the soft robotic arm and carry out a trajectory planning experiment. The target trajectory is an 8-shaped spatial curve at the projection onto the XOY plane. We choose 41 waypoints from it. According to the BP network prediction model and the analytical model in section II, we can calculate the corresponding input pressure vectors with different methods. In Fig. 10(a) and (b), the input signals of three-chamber pressure used to complete the trajectory are given.

Fig. 10(c) to (f) shows the path at the tip of the SBA under input pressure vectors, the target route point selected to calculate the required pressure, and the actual route point in the top view and the side view, respectively. The position error while following the path is shown in Fig. 11. For the 41 waypoints, the average position error, the standard deviation, and the maximum value are given in Table I. The mean relative error relative to the total arm length is 2.46 %. Compared with the relative average error of 3.09% with respect to the total length of the soft actuator in the national analytical model, the experimental results demonstrate that the developed BP network model has more accuracy.

The performance of the model in the trajectory planning experiment is not perfect. The reasons for measurement error are analyzed. On the one hand, an open-loop static controller is not suitable enough for continuously moving control; on the other hand, the hysteresis of soft materials and the pulse shock signal of proportional valves lead to errors.

Nevertheless, the results achieved in this work open a set of future investigations in the control of soft robots implementing more advanced machine learning methods.

V. CONCLUSIONS AND FUTURE WORK

In this study, we demonstrate a three-chamber pneumatic soft actuator that has a modular structure and present its design and fabrication. Although some kinematic model studies have been carried out on the three-chamber soft actuator, it is difficult to get the exact solutions by a traditional analytical model. Few people combine the BP

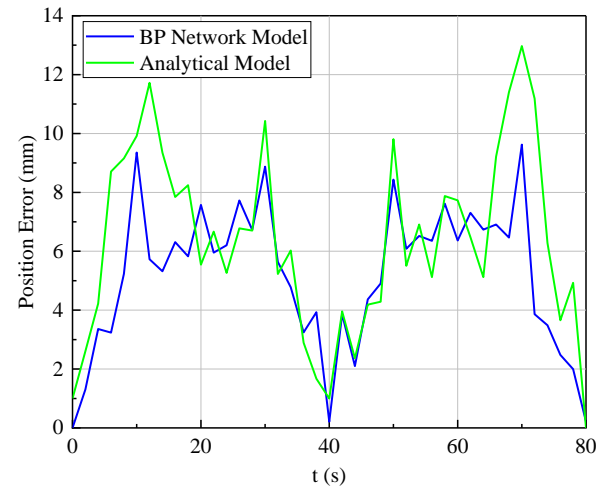


FIGURE 11. The experimental procedure followed in the model application section.

TABLE I
DIMENSIONS OF EXPERIMENT ERRORS

| Symbol | BP network model | Analytical model |
|----------------------------|------------------|------------------|
| Average position error[mm] | 5.17 | 6.34 |
| Maximum position error[mm] | 9.35 | 12.96 |
| Standard deviation | 0.38 | 0.49 |

neural network with the kinematic model. Thus, this article puts forward a scheme aided by BP neural network modeling to realize nonlinear prediction and mapping from the tip coordinates (x, y, z) to the input pressures.

Thus, the conclusions can be summarized as follows:

1) Based on the BP neural network algorithm, a complete soft biomimetic actuator inverse kinematics framework that can predict the driving pressures of the SBA on curved trajectories is developed. By solving the model, we find the optimal parameters of the BP network computing framework for high-required precision.

2) The feasibility of the prediction model based on the BP neural network has been tested on the real soft biomimetic arm. The prediction model shows accurate and fast performance because the mean position error is 5.17 mm, the maximum position error is 9.35 mm, and the standard deviation is 0.38. The mean relative error relative to the total arm length is 2.46 %. All these error dimensions are less than those of a traditional analytical method.

The performance result of the model in the model application section is imperfect. The current problem is that this BP neural network model is an open-loop static controller, which is not suitable enough for continuous control. In addition, the manufacturing error and environmental change greatly affect the motion results of the soft biomimetic robotic arm. For future work, the combination of feedback control and damping is expected to achieve more precise control of the complex motion.

Subsequently, the hybrid intelligence algorithm (e.g., combining BP neural network and genetic algorithms) is hopeful to further improve the accuracy of the inverse kinematics prediction of a soft biomimetic actuator. To explore the universality of this method, it will be validated with more complex soft actuators. The soft biomimetic robotic arm can be put to wide use in searching and rescuing in narrow workspaces, medical applications in long-distance surgical operations, and underwater operations.

ACKNOWLEDGMENT

A preprint has previously been published[37].

REFERENCES

- [1] D. Rus and M. T. Tolley, "Design, fabrication and control of soft robots," *Nature*, vol. 521, no. 7553, pp. 467-475, 2015.
- [2] H. Ma and J. Zhou, "A Multi-Physics Simulation Approach to Predict Shape Morphing of Flexible Devices in Magnetic Field," in *2021 IEEE International Conference on Mechatronics and Automation (ICMA)*, Aug. 8-11 2021, pp. 344-349, doi: 10.1109/ICMA52036.2021.9512696.
- [3] T. Mahl, A. Hildebrandt, and O. Sawodny, "A Variable Curvature Continuum Kinematics for Kinematic Control of the Bionic Handling Assistant," *IEEE Trans. Rob.*, vol. 30, no. 4, pp. 935-949, 2014.
- [4] Z. Zhang, H. Chen, and Z. Zhang, "Configuration Synthesis and Performance Analysis of Finger Soft Actuator," *Applied Bionics and Biomechanics*, vol. 2018, p. 4264560, 2018.
- [5] G. Li *et al.*, "Self-powered soft robot in the Mariana Trench," *Nature*, vol. 591, no. 7848, pp. 66-71, 2021.
- [6] J. Z. Gul, B.-S. Yang, Y. J. Yang, D. E. Chang, and K. H. Choi, "In situUV curable 3D printing of multi-material tri-legged soft bot with spider mimicked multi-step forward dynamic gait," *Smart Mater. Struct.*, vol. 25, no. 11, p. 115009, 2016.
- [7] G. Thiruthel Thomas, B. Shih, C. Laschi, and T. Tolley Michael, "Soft robot perception using embedded soft sensors and recurrent neural networks," *Sci. Robot.*, vol. 4, no. 26, p. eaav1488, 2019.
- [8] P. Cheng, Y. Ye, J. Jia, C. Wu, and Q. Xie, "Design of cylindrical soft vacuum actuator for soft robots," *Smart Mater. Struct.*, vol. 30, no. 4, p. 045020, 2021.
- [9] V. Cacucciolo, F. Renda, E. Poccia, C. Laschi, and M. Cianchetti, "Modelling the nonlinear response of fibre-reinforced bending fluidic actuators," *Smart Mater. Struct.*, vol. 25, no. 10, p. 105020, 2016.
- [10] M. A. Robertson and J. Paik, "New soft robots really suck: Vacuum-powered systems empower diverse capabilities," *Sci. Robot.*, vol. 2, no. 9, 2017.
- [11] C. D. Onal and D. Rus, "A modular approach to soft robots," in *2012 4th IEEE RAS & EMBS International Conference on Biomedical Robotics and Biomechatronics (BioRob)*, 24-27 June 2012 2012, pp. 1038-1045, doi: 10.1109/BioRob.2012.6290290.
- [12] Y. F. Zhang *et al.*, "Fast - Response, Stiffness - Tunable Soft Actuator by Hybrid Multimaterial 3D Printing," *Advanced Functional Materials*, vol. 29, no. 15, p. 1806698, 2019.
- [13] C. Laschi, B. Mazzolai, V. Mattoli, M. Cianchetti, and P. Dario, "Design of a biomimetic robotic octopus arm," *Bioinspir. Biomim.*, vol. 4, no. 1, p. 015006, 2009.
- [14] B. Mazzolai, L. Margheri, M. Cianchetti, P. Dario, and C. Laschi, "Soft-robotic arm inspired by the octopus: II. From artificial requirements to innovative technological solutions," *Bioinspir. Biomim.*, vol. 7, no. 2, p. 025005, 2012.
- [15] L. Xu *et al.*, "Bio-inspired annelid robot: a dielectric elastomer actuated soft robot," *Bioinspir. Biomim.*, vol. 12, no. 2, p. 025003, 2017.
- [16] C. Laschi, B. Mazzolai, and M. Cianchetti, "Soft robotics: Technologies and systems pushing the boundaries of robot abilities," *Sci. Robot.*, vol. 1, no. 1, 2016.
- [17] M. Giorelli, F. Renda, M. Calisti, A. Arienti, G. Ferri, and C. Laschi, "A two dimensional inverse kinetics model of a cable driven manipulator inspired by the octopus arm," in *2012 IEEE International Conference on Robotics and Automation*, May. 14-18 2012, pp. 3819-3824, doi: 10.1109/ICRA.2012.6225254.
- [18] M. Giorelli, F. Renda, G. Ferri, and C. Laschi, "A feed-forward neural network learning the inverse kinetics of a soft cable-driven manipulator moving in three-dimensional space," in *2013 IEEE/RSJ International Conference on Intelligent Robots and Systems*, 3-7 Nov. 2013 2013, pp. 5033-5039, doi: 10.1109/IROS.2013.6697084.
- [19] A. Martín, A. Barrientos, and J. del Cerro, "The Natural-CCD Algorithm, a Novel Method to Solve the Inverse Kinematics of Hyper-redundant and Soft Robots," *Soft Rob.*, vol. 5, no. 3, pp. 242-257, 2018.
- [20] J. Zhang, J. Zhou, Z. K. Cheng, and S. Yuan, "Fabrication, Mechanical Modeling, and Experiments of a 3D-Motion Soft Actuator for Flexible Sensing," *IEEE Access*, vol. 8, pp. 159100-159109, 2020.
- [21] A. D. Marchese and D. Rus, "Design, kinematics, and control of a soft spatial fluidic elastomer manipulator," *Int J Rob Res*, vol. 35, no. 7, pp. 840-869, 2015.
- [22] A. Shiva *et al.*, "Elasticity Versus Hyperelasticity Considerations in Quasistatic Modeling of a Soft Finger-Like Robotic Appendage for Real-Time Position and Force Estimation," *Soft Rob.*, vol. 6, no. 2, pp. 228-249, 2019.
- [23] A. D. Marchese, R. Tedrake, and D. Rus, "Dynamics and trajectory optimization for a soft spatial fluidic elastomer manipulator," *Int J Rob Res*, vol. 35, no. 8, pp. 1000-1019, 2015.
- [24] I. S. Godage, G. A. Medrano-Cerda, D. T. Branson, E. Guglielmino, and D. G. Caldwell, "Dynamics for variable length multisegment continuum arms," *Int J Rob Res*, vol. 35, no. 6, pp. 695-722, 2015.
- [25] R. J. Webster and B. A. Jones, "Design and Kinematic Modeling of Constant Curvature Continuum Robots: A Review," *Int J Rob Res*, vol. 29, no. 13, pp. 1661-1683, 2010.
- [26] L. Marechal, P. Balland, L. Lindenroth, F. Petrou, C. Kontovounios, and F. Bello, "Toward a Common Framework and Database of Materials for Soft Robotics," *Soft Rob.*, vol. 8, no. 3, pp. 284-297, 2020.
- [27] Y. Sun, H. Feng, I. R. Manchester, R. C. H. Yeow, and P. Qi, "Static Modeling of the Fiber-Reinforced Soft Pneumatic Actuators Including Inner Compression: Bending in Free Space, Block Force, and Deflection upon Block Force," *Soft Rob.*, 2021.
- [28] G. Fang, C. D. Matte, R. B. N. Scharff, T. H. Kwok, and C. C. L. Wang, "Kinematics of Soft Robots by Geometric Computing," *IEEE Trans. Rob.*, vol. 36, no. 4, pp. 1272-1286, 2020.
- [29] K. Elgeneidy, N. Lohse, and M. Jackson, "Bending angle prediction and control of soft pneumatic actuators with embedded flex sensors – A data-driven approach," *Mechatronics*, vol. 50, pp. 234-247, 2018.
- [30] I. M. Van Meerbeek, C. M. De Sa, and R. F. Shepherd, "Soft optoelectronic sensory foams with proprioception," *Sci. Robot.*, vol. 3, no. 24, 2018.
- [31] J. Y. Loo, Z. Y. Ding, V. M. Baskaran, S. G. Nurzaman, and C. P. Tan, "Robust Multimodal Indirect Sensing for Soft Robots Via Neural Network-Aided Filter-Based Estimation," *Soft Rob.*, 2021.
- [32] K. Nakajima, H. Hauser, T. Li, and R. Pfeifer, "Exploiting the Dynamics of Soft Materials for Machine Learning," *Soft Rob.*, vol. 5, no. 3, pp. 339-347, 2018.
- [33] Y. Wang, A. Sha, X. Li, and W. Hao, "Prediction of the Mechanical Properties of Titanium Alloy Castings Based on a Back-Propagation Neural Network," *J. Mater. Eng. Perform.*, 2021.
- [34] H. Yu and T. Wang, "A Method for Real-Time Fault Detection of Liquid Rocket Engine Based on Adaptive Genetic Algorithm Optimizing Back Propagation Neural Network," *Sensors*, vol. 21, no. 15, 2021.
- [35] W. Z. Xu Dong, *Analysis and Design -Neural Network Based on MATLAB6. x (second edition)*. Xi'an University of Electronic Science and Technology Publishing Press, 2002, p. 152.
- [36] Q. Xie, T. Wang, S. Yao, Z. Zhu, N. Tan, and S. Zhu, "Design and modeling of a hydraulic soft actuator with three degrees of freedom," *Smart Mater. Struct.*, vol. 29, no. 12, p. 125017, 2020.
- [37] J. Z. Huichen Ma, Jian Zhang, Lingyu Zhang, "Research on the inverse kinematics prediction of a soft actuator via BP neural network," unpublished.